Radiological Anatomy and Approaches to the Spine

3

Alvaro Antonio Diano, Gianluigi Guarnieri and Mario Muto

3.1 Introduction

The fundamental concept of normal anatomy of the spine is crucial for a correct approach to minimally invasive spinal treatments. In this chapter, the spinal anatomy and paravertebral soft tissue will be discussed because they represent the "roadmap" during the percutaneous procedures carried out under fluoroscopic or computed tomography (CT) guidance.

The goal of a minimally invasive interventional procedure in the spine (irrespective of which one is employed) is to reach a particular "target" located in the vertebral body (VB) or the posterior arch by the least traumatic and safest way possible. However, the approach must permit valid diagnostic or therapeutic results.

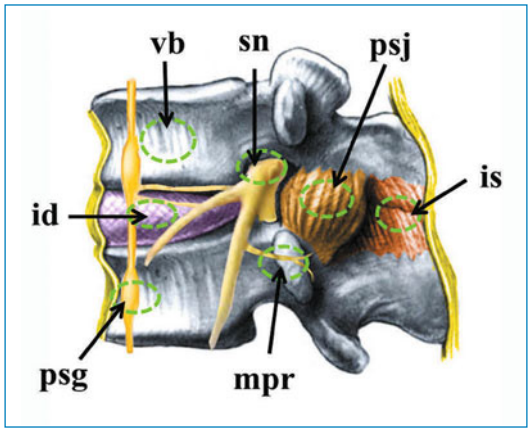

Fig. 3.1 Main targets of percutaneous interventional procedures in the spine. Vertebral body (*vb*); intervertebral disks (*id*); ganglion and spinal nerve (*sn*); paraspinal sympathetic ganglion (*psg*); posterior spinal facet joint (*psj*); interspinous space (*is*); medial branch posterior ramus (*mpr*)

3.2 General Points to Consider

The *rationale* of percutaneous treatment is to reach a specific target under radiographic guidance in the safest possible way. It is possible to design precisely the route to reach the anatomical location desired, as well as constant monitoring during execution of the procedure and the immediate verification of the results obtained.

In the specific case of the spine, the target is anatomical landmarks such as facet joints, intervertebral disks, posterior arch, lamina, and paraspinal nerve structures (Fig. 3.1). These regions are readily identified by fluoroscopy or CT. Fluoroscopy is characterized by a wide field of view and sufficient spatial resolution only on skeletal parts. CT also provides detailed information on soft paravertebral tissue (especially on muscle or fatty tissue and often about vascular and nerve structures). To carry out minimally invasive percutaneous procedures, summarizing

M. Muto (✉)
Neuroradiology Department, A. Cardarelli Hospital, Naples, Italy
e-mail: mutomar2@gmail.com

M. Muto (ed.), *Interventional Neuroradiology of the Spine,*
DOI 10.1007/978-88-470-2790-9_3, © Springer-Verlag Italia 2013

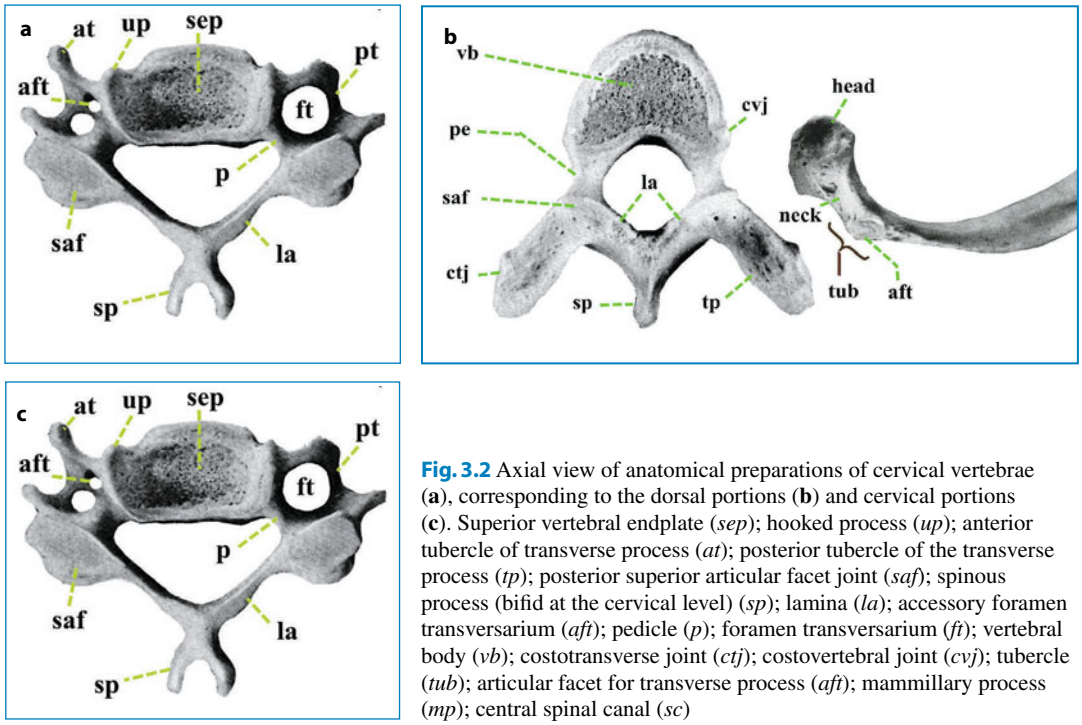

Fig. 3.2 Axial view of anatomical preparations of cervical vertebrae (**a**), corresponding to the dorsal portions (**b**) and cervical portions (**c**). Superior vertebral endplate (*sep*); hooked process (*up*); anterior tubercle of transverse process (*at*); posterior tubercle of the transverse process (*tp*); posterior superior articular facet joint (*saf*); spinous process (bifid at the cervical level) (*sp*); lamina (*la*); accessory foramen transversarium (*aft*); pedicle (*p*); foramen transversarium (*ft*); vertebral body (*vb*); costotransverse joint (*ctj*); costovertebral joint (*cvj*); tubercle (*tub*); articular facet for transverse process (*aft*); mammillary process (*mp*); central spinal canal (*sc*)

the normal spinal anatomy and radiographic elements of the spine is important.

3.3 Normal Anatomy of the Spine

The spinal column is divided in five segments: cervical, thoracic, lumbar, sacral and coccyx. The spinal column comprises thirty-three individual segments: the vertebrae. They consist of an anterior bony block, the body and a posterior element, as well as the neural arch (which contains the articular, transverse and spinous processes). The VB is a cylindrical formation of cancellous bone enclosed in a thin shell of compact bone, which is in correspondence with the upper and lower surface.

The basic architecture is similar in the different regions of the spinal column. However, the mass and size of the vertebrae increases gradually proceeding from the first cervical vertebra up to the last lumbar vertebra as a natural adaptation in response increases in mechanical loading. Other major differences are the presence of the foramina for both vertebral arteries in the transverse processes at the cervical level, the facet joints in the ribs at the thoracic vertebrae, and the mammary processes at the lumbar level (Fig. 3.2).

The first two cervical vertebrae are considerably different from the others. The atlas (C1) does not have an anterior body. It corresponds to the odontoid process of the second cervical vertebra and is formed by an anterior arch that is joined to the posterior arch by two lateral masses (the articular processes) to which there are the transverse processes. The surface of the upper articular processes has an ellipsoid, irregular and concave shape (Fig. 3.3) with an axis directed forward and laterally (the inclination is about 40° from the median sagittal plane), also known as the "glenoid cavity", that receives the occipital condyles.

The posterior arch corresponds to the lamina of the remaining vertebrae where, on its upper surface, is located the sulcus for the vertebral artery. The posterior tubercle is the vestigial remnant of the spinous processes. The second cervical vertebra is characterized by the odontoid process or dens, which is derived from the central nucleus of ossification of the atlas (C1). The dens

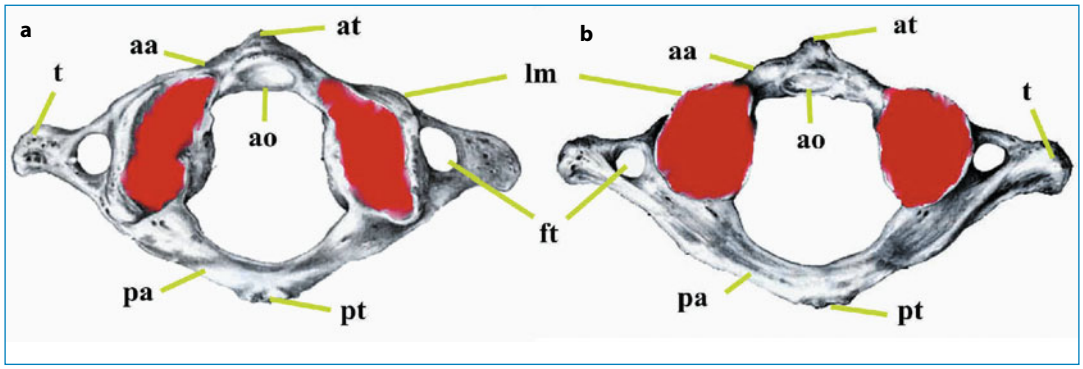

Fig. 3.3 The atlas. Upper (**a**) and lower view anatomical detail (**b**). Articular surface for odontoid process of C2 (*o*); anterior arch (*aa*); posterior neural arch (lamina) (*pa*); lateral mass (*lm*) for vertebral artery foramen transversarium/ veins (*ft*); posterior tubercle (*pt*); anterior tubercle (*Pt*); transverse process (*t*)

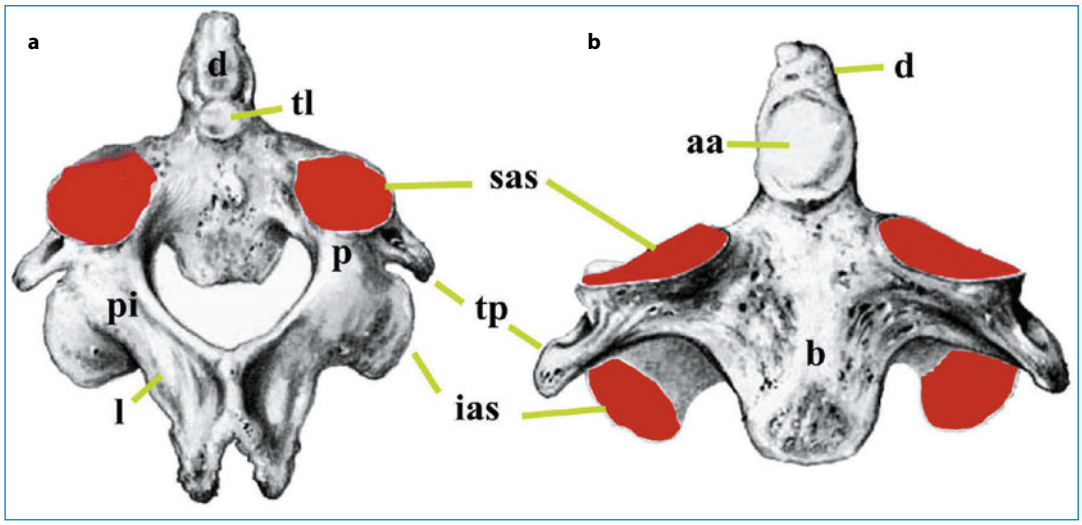

Fig. 3.4 Axis. Anatomical detail of C2: three quarters posterior superior view (**a**) and frontal view (**b**). Dens (*d*); point of insertion of transverse axial ligament (posterior articular facet) (*tl*); anterior articular facet for median atlanto-axial joint (*aa*); superior articular facet (*sas*); inferior articular facet (*ias*); pars interarticularis (*pi*); pedicle (*p*); lamina (*L*); transverse process (*tp*); body of C2 (*b*)

is a bony, conical-shaped process that extends up almost to the inferior end plate of the clivus and is provided with two articular facets: a ventral one in contact with the anterior arch of the atlas and a dorsal one that comes into contact with the transverse ligament (Fig. 3.4). By each side of the dens are two articular apophyses which support the weight of the head.

The upper facet joints overflow outside, below and behind with respect to the body of C2, standing midway between the two structures on which the load is shared: the diskal and articular processes. Their surface is flat in the transverse direction but can be also slightly convex, and they have a thin edge of compact bone along which a ring on left lateral (LL) radiographic projection can be defined. The peduncles are particularly large, more vertical and less oriented with respect to other cervical vertebrae, and delimit the vertebral artery canal. The posterior arch appears to be disproportionate with respect to the body because it must distribute the forces of the muscle inserted on the spinous C2 apophysis. The transverse processes are short, the laminae have a

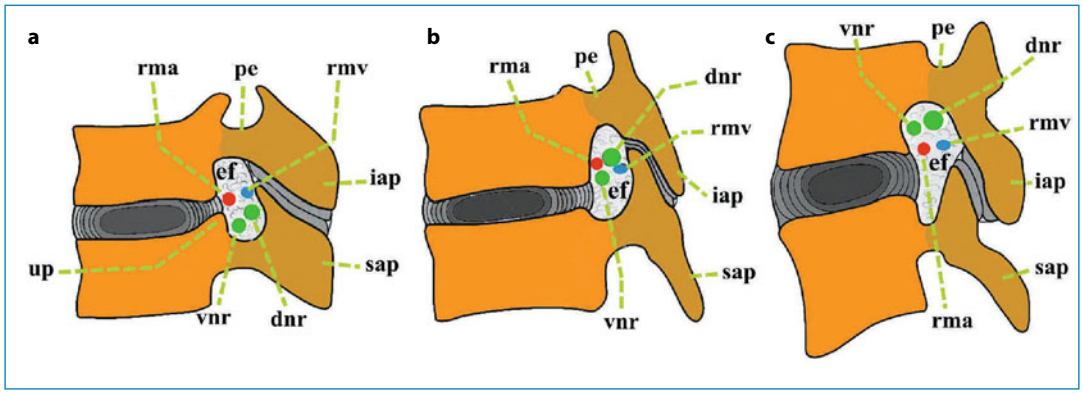

Fig. 3.5 Schematic view in the sagittal section of the foramen and nerve vascular structures at cervical (**a**), thoracic (**b**) and lumbar (**c**) levels. Ventral nerve root (*vnr*); dorsal nerve root (*dnr*); epidural fat (*f*); hooked process (*up*); radiculomedullary artery (*rma*); radiculomedullary vein (*rmv*); superior articular process (*sap*); inferior articular process (*iap*), pedicle (*pe*)

rectangular shape, and the spinous processes are often long and stout [1–7]

To carry out minimally invasive interventional procedures, knowing four key spinal elements is important: neural foramen, posterior facet joints, sympathetic nervous system, and the spinal nerve.

3.3.1 Neural Foramen

The neural foramen is also called the "intervertebral foramen". It contains primarily the nerves (with an anterior motor root and posterior sensitive root plus its ganglion), the vascular structures, and some fatty cells primarily distributed in its upper portion. The neural foramen is delimited: by the articular process posteriorly; by the VB with the disk anteriorly; on the upper side by the inferior margin of the pedicle of the cranial vertebra; and inferiorly by the upper margin of the pedicle of the vertebra below. At the cervical level, the anterior nerve root is related to the unciform processes and the vertebral artery. At the cervical level, the nerve root occupies the lower part of the foramen, whereas in the upper portion are placed the vessels and fat (Fig. 3.5a). At the thoracic level, the nerves and vessels are in the middle portion of the foramen (Fig. 3.5b). At the lumbar level they are in the upper portion of the foramen (Fig. 3.5c).

These neural elements (particularly those at the cervical level) are surrounded by numerous veins that, on CT after injection of contrast media, permit recognition of the epidural space, allowing identification of the structures contained therein. The cervical nerve roots are numbered from C1. The first nerve root leaves the spinal canal at the space between the occipital bone and C1, up to the C8 nerve root that emerges from the neural foramen of C7–D1. Consequently, the numbering of the nerve roots in the remaining thoracic and lumbar segments is staggered by one level down compared with the corresponding VB (the twelfth thoracic nerve engages the intervertebral foramen D12–L1, whereas the fifth lumbar nerve engages the foramen L5–S1). The extent of inclination of the foramina changes in the various segments of the spine compared with the sagittal plane. The channel is directed obliquely in the anterolateral side in the cervical and laterally in the thoracolumbar level [8–9] (Fig. 3.6).

3.3.2 Posterior Facet Joints

At the cervical level, the articular apophyses have a cylindrical shape with an angle of 45° with respect to the horizontal plane. On their surface are the facet joints, which are inclined downwards by about 45°. Because of their spatial orientation they seem to have a "parallelogram" appearance

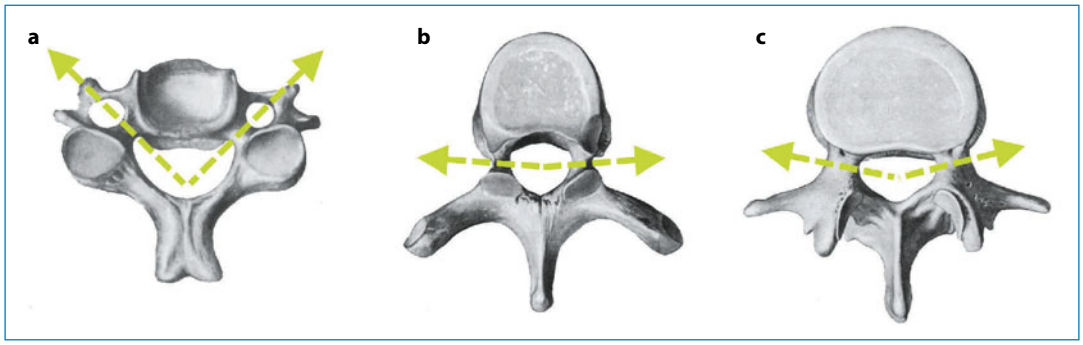

Fig. 3.6 Orientation in the axial plane of the channel of conjugation in the cervical (**a**), thoracic (**b**) and lumbar (**c**) levels

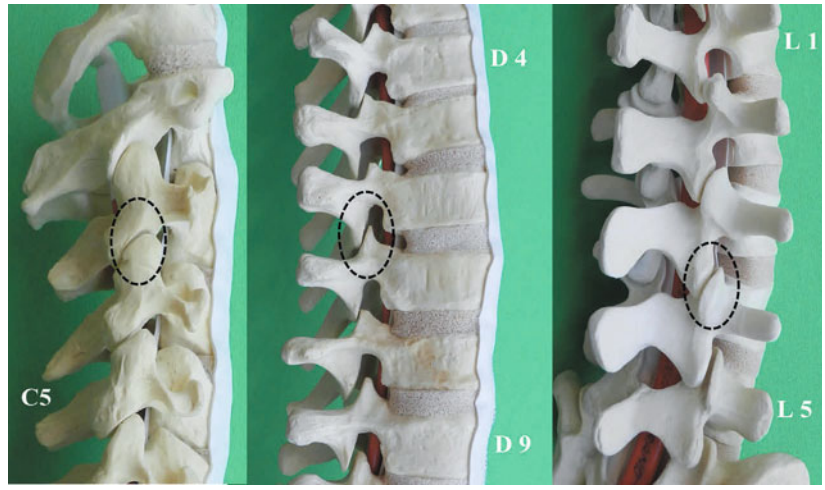

Fig. 3.7 Lateral view of cervical and thoracic spinal segments and oblique view of lumbar segments with demonstration of the facet joints

with a cone shape on the LL view on radiographs, whereas on all other radiographic projections they assume an oval appearance with margins that are more or less rounded. At the thoracic level, the facet joints have a flat surface and are directed back and forth over the lower ones. At the lumbar level, the articular processes appear as flattened bone formations located at the junction between the lamina and pedicles and posteriorly with respect to the transverse processes. The superior articular apophyses have an internal joint surface in the form of a vertical shower, covered with cartilage. Their outer surface shows a small bone on the back edge called the mammillary tubercle. The inferior articular apophyses are implanted on the lower edge of the lamina, and are directed obliquely downwards and backwards.

The convex articular surface of the inferior articular apophyses is in contact with the upper articular apophysis of the vertebra below. At the sagittal plane they form an angle that increases progressively from L1 to L5, being nearly a sagittal line from L1 to L4 and almost a frontal line at L4–L5 and L5–S1. However, the orientation changes from one subject to another or in the same subject, and often there is an asymmetry between the two sides. At the L4–L5 and L5–S1 joint space, the right side is more sagittal than the left in 70% of cases [10–13]. In the sagittal plane, the orientation of the joint is almost vertical (Fig. 3.7). To understand the important role of this articulation during interventional procedures, its anatomy must be specified. The interapophyseal articulation is a synovial joint that is often associated (as with all other joints) with inflammatory–degenerative processes. The folds of the synovial membrane may extend between the articular surfaces and cause pain if they are inflamed. The articular surfaces are covered with

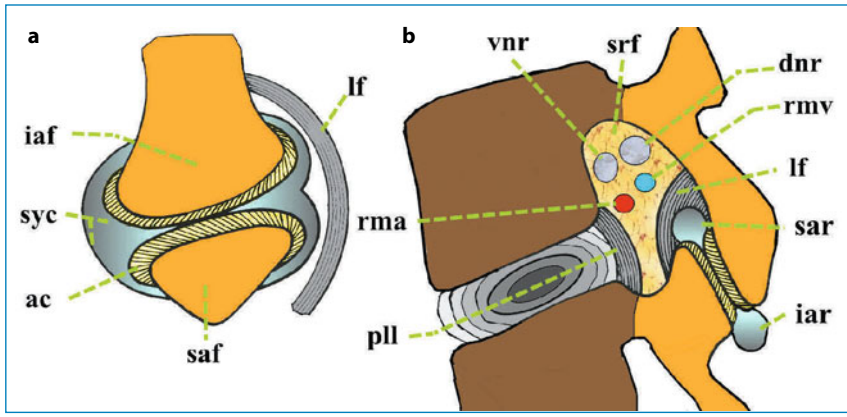

Fig. 3.8 Schematic view of the inter-apophysis junction at the lumbar level in axial (**a**) and sagittal (**b**) sections. Ligamentum flavum (*lf*); posterior superior articular facet joint surface (*saf*); posterior inferior articular facet joint surface (*iaf*); articular cartilage (hyaline) of facet joint (*ac*); synovial membrane and capsular ligament of posterior spinal joint face (*syc*); superior articular recess (*sar*); inferior articular recess (*iar*); superior recess of the neural foramen (*srf*); dorsal nerve root (*dnr*); ventral nerve root (*vnr*); radiculomedullary artery (*rma*); radiculomedullary vein (*rmv*); posterior longitudinal ligament (*pll*)

hyaline cartilage, interlock with each other, and are joined together by the joint capsule. In general, the interarticular space is curved from front to back and forwards and outwards. The articular apophyses are enclosed in a capsule, and are reinforced by the lateral segment of the ligamentum flavum and by the posterior ligament. There are two joint recesses: the higher one is located anteriorly and is in proximity to the spinal canal and neural elements, and can be up to the neural foramen (Fig. 3.8).

Two other small recesses can be found. They are inconstant and extend the full height of the joint: the anterior-medial recess and posterolateral recess [14]. The size of the inferior recess varies based on the static lumbar spine. An increase in lumbar lordosis tends to widen the upper recess, whereas an increase in kyphosis determines a wider inferior recess. Hence, it is desirable to place a pillow under the abdomen of the patient to reduce the lordosis and facilitate puncture of the inferior recess.

The innervation of the posterior vertebral joints is rich and complex (Fig. 3.9). On each side there is a sensory nerve from the ipsilateral posterior branch of the same level of the spinal nerve, and sensory branches of the spinal nerve arise from those above.

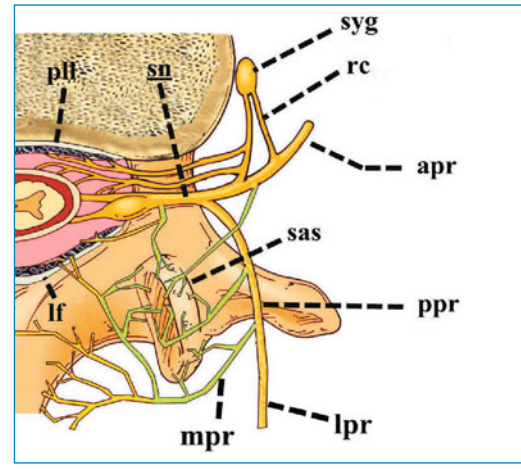

Fig. 3.9 Innervation of the facet joints and spinal nerve. The nerve branches directed to the articular apophyses are highlighted. Sympathetic ganglion (*syg*); branches comunicantes (*rc*); anterior primary ramus (*apr*); posterior primary ramus (*ppr*); medial branch posterior ramus (*mpr*); ramus posterior lateral branch (*lpr*); posterior longitudinal ligament (*pll*); ligamentum flavum (*lf*); superior articular facet (*sas*); spinal nerve (*sn*)

3.3.3 Sympathetic Nervous System in the Spine

Pre-ganglion cells of the anterior horn of the nerve fibers of the spinal cord originate in the passing ventral root of the spinal nerve and are

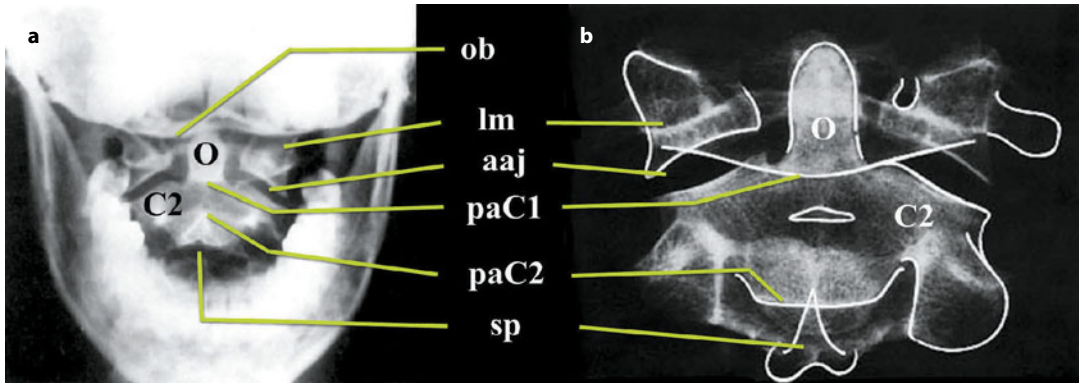

Fig. 3.10 Plain radiograph (anteroposterior projection) of the occipito-vertebral hinge (**a**) and anatomical preparation of dry bone (**b**). Odontoid process (dens) (*O*); body of C2 (*C2*); occipital bubble (*b*); lateral mass of C1 (*lm*); atlanto-axial joint (*aaj*); posterior arch of C1 (*inferior edge*); posterior arch of C2 (*superior edge*); spinous process of C2 (*sp*)

conveyed through gray communicating branches to form a sympathetic chain. Their nerve impulses produce contraction of smooth muscle cells (e.g., the muscular coats of the intestine, bronchi, vessels), and determine the secretory effects (glands) or trophic effects on the connective tissue of the organs. The two chains of sympathetic ganglia or trunks located in the paravertebral space extend from the base of the skull to the coccyx and divide into complexes. A detailed description of the sympathetic chain and spinal nerve is beyond the scope of this chapter.

3.4 Radiographic Anatomy of the Spine

3.4.1 Cervical Spine

The radiographic study is undertaken with a transoral projection for the first two cervical vertebrae and with the anteroposterior (AP), LL and oblique projections for the lower cervical segments.

In the transoral projection it is possible to reduce the overlap of most of the skeletal structures of the face. The central X-ray beam affects the center of the mouth and flows out to the height of the inion (or just below). The degree of forward head tilt should be well balanced because it can cause a pronounced overlap of the upper alveolar processes of the teeth, and a slight extension can cause a similar overlap due to the occipital bone. Anatomical radiographic findings start from the midline and proceed outwards: the odontoid process, the lateral masses of the atlas, and the transverse processes of the atlas. The inferior articular facets of C1 are increasingly evident with a well-defined lower edge and acute infero-external angle. The anterior lamina of C1 is projected on the lateral mass as an opaque ring. On the inner face of the lateral masses, tubercles that give attachments to the transverse ligament are clearly visible. The C2 pedicles are projected onto the VB with an external concavity. The posterior arch of C2 is evident through the body as well as the spinous process. The superior articular facets of C1 and the occipital condyles are more or less evident in relation to the maxilla and occipital bone (Fig. 3.10).

The cervical spine from C3 to C7 can be examined with three projections: AP; LL; and right and left 45° oblique.

AP projection: The cervical spine from C3 to T1 is represented, and shows the VBs, interbody space, unciform apophyses and uncovertebral joints (Fig. 3.11). Because of their orientation, the peduncles are not clearly shown in AP projection. They are reduced to two small opacities situated at the sides of the body which can be appreciated only in the upper and lower outlines. In general, it is not possible to distinguish the upper and lower edges of the posterior arch, of which only the spinous process is evident. Due to their orienta-

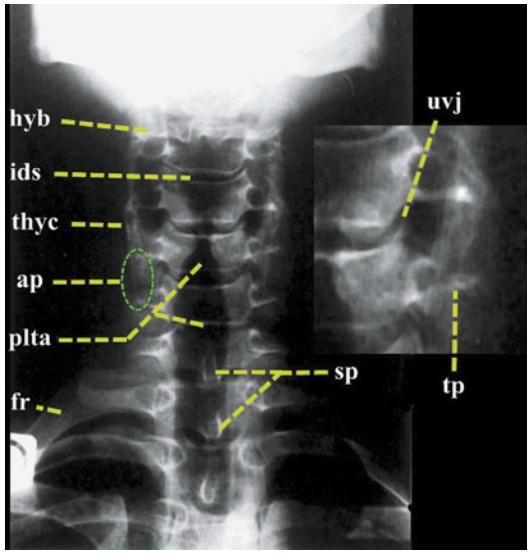

Fig. 3.11 Conventional radiographic anatomy of the cervical spine in the anteroposterior projection. Hyoid bone (*hyb*); uncovertebral joint (*uvj*); intervertebral disk space (*ids*); thyroid cartilage (*thyc*); laryngo–pharyngo–tracheal airway (*plta*); tansverse process (*tp*); articular process (*ap*); spinous process (*sp*); first rib (*fr*)

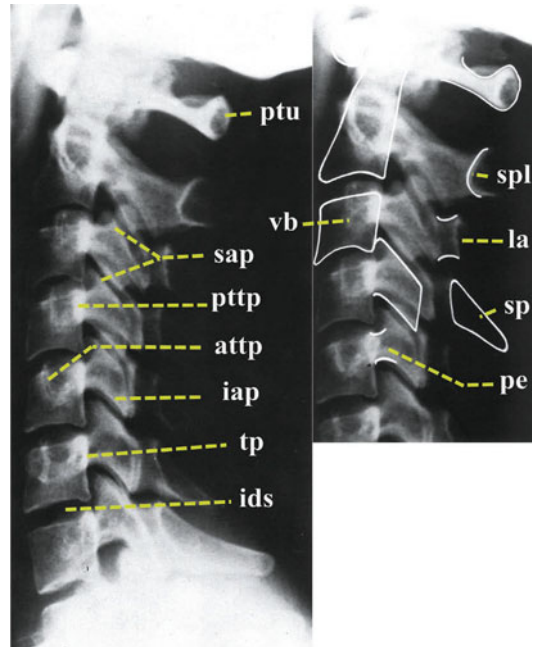

Fig. 3.12 Plain radiograph (left lateral projection) of the cervical spine. Posterior tubercle of the posterior arch of C1 (*ptu*); posterior tubercle of the transverse process (*pttp*); anterior tubercle of the transverse process (*attp*); superior articular process of the posterior spinal facet joint (zygapophyseal) (*sap*); inferior articular process of the posterior spinal facet joint (zygapophyseal) (*iap*); lamina (*la*); pedicle (*pe*); spinolaminar line (*spl*); transverse process (*tp*); intervertebral disk space (*ids*); spinous process (*sp*); vertebral body (*vb*) (C3)

tion and subtlety, the articular apophyses are not clearly visible and appear as an "elephant's ear". Only the VBs are clearly visible along with the uncus and uncovertebral joints. The articular processes are overlapped as a double opacity with a vertical course, almost constant, at the sides of the soma. The first ribs and first dorsal vertebrae can be seen clearly. False images at the C4 and C5 levels can be created due to: the transparency of the tracheo–pharyngeal–laryngeal axis; the epiglottis; the opacity of the larynx cartilage; the hyoid bone; overlapping of the spine.

LL projection: VBs and the interbody space can be assessed on the LL projection. With regard to the atlas, the profile of the anterior arch (like a signet ring) and the posterior arch (in which the cortex is very clear) can be evaluated clearly.

The space between the odontoid and anterior arch of the atlas is usually ≤2.5 mm in adults. The lateral masses of the atlas are projected on the odontoid and, in general, are poorly analyzed. The posterior margin of the soma of C2 is in continuity with that of the dens, but sometimes it can form an angle as an anatomical variant. In the section below the atlo-occipital joint, the VBs have a rectangular appearance with an antero-inferior "beak" with overlapping of the transverse process. Posterior to the body are the articular processes with a parallelogram shape. Posterior to the articular processes are projected the laminae, which form the "spinolaminar space" (used to evaluate stenosis of the spinal canal). Behind the laminae are the spinous processes, non-existent only for C1, whereas they are more developed from C6 to C7 (Fig. 3.12).

The 45° oblique projection is used to evaluate the conjugation foramen, so the orientation of the X-ray beam must be the same as that of the conjugation foramen: 40° in relation to the frontal plane and 15–20° in relation to the horizontal

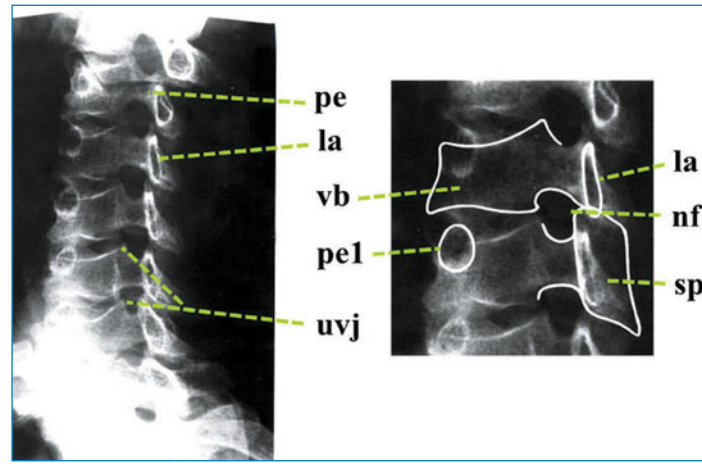

Fig. 3.13 Plain radiograph (oblique projection) of the cervical spine. Pedicle (*pe*); lamina (*la*); vertebral body (*vb*); neural foramen (*nf*); spinous process (*sp*); pedicle side in the examination (*pe1*); uncovertebral joint (*uvj*)

plane. In this projection, the foramina have an oval shape that is delimited anteriorly by the posterolateral angle of the VBs, disk and uncus, and posteriorly by and the articular apophysis. The peduncles can be seen clearly; those which are ipsilateral are seen according to their major axis. The contralateral laminae are projected in the foramen whereas the ipsilateral laminae appear as vertical opacities. The facet joints are not seen clearly: they appear as partially overlapping oval formations. More posteriorly, spinous processes can be observed [2] (Fig. 3.13).

3.4.2 Thoracic Spine

The radiographic views used to study the thoracic spine, unlike the other segments of the spine, are the AP and LL projections. In some cases, these projections are supplemented by detailed projections studying the VBs and interbody space.

AP projection (Fig. 3.14a): VBs are rectangular and their volume increases progressively if proceeding in a caudal direction. The endplates are regular but the lateral edges are slightly concave. The peduncles are of very variable form, often rounded, and projected in the top half of the vertebral VB near the lateral angle. They are quite small at the level of the first thoracic vertebrae and reach maximum size at the T11–T12 level. The inter-pedicular distance remains almost constant throughout the thoracic spine. The spinous processes are projected onto the VB below. The intervertebral space has a nearly constant height throughout the thoracic segment. The anatomical structures that are most difficult by radiography are the: upper edges of the laminae (on AP projection they overlap with the superior endplate of the vertebra below because they are concave); upper and lower facet joints; transverse processes (which are masked by overlapping of the head of the ribs).

LL projection (Fig. 3.14b): VBs are rectangular and the endplates slightly concave. The front edge of the soma is vertical or slightly concave, the back wall is straight and less defined. The peduncles are implanted on the upper half of the VB and have an upper edge that is almost in continuity with the upper somatic plate; the lower edge is concave. The shape of the neural foramina is oval. The articular apophysis is just behind the foramina as an isosceles triangle. The interbody spaces for each level are the same height from back to front and increase up to the lumbar level. The spinous processes as well as the transverse and inferior articular processes are more difficult to analyze because of the overlap of the ribs and lungs [10].

3.4.3 Lumbar Spine

AP projection: VBs have a rectangular shape with straight endplates and lateral margins that

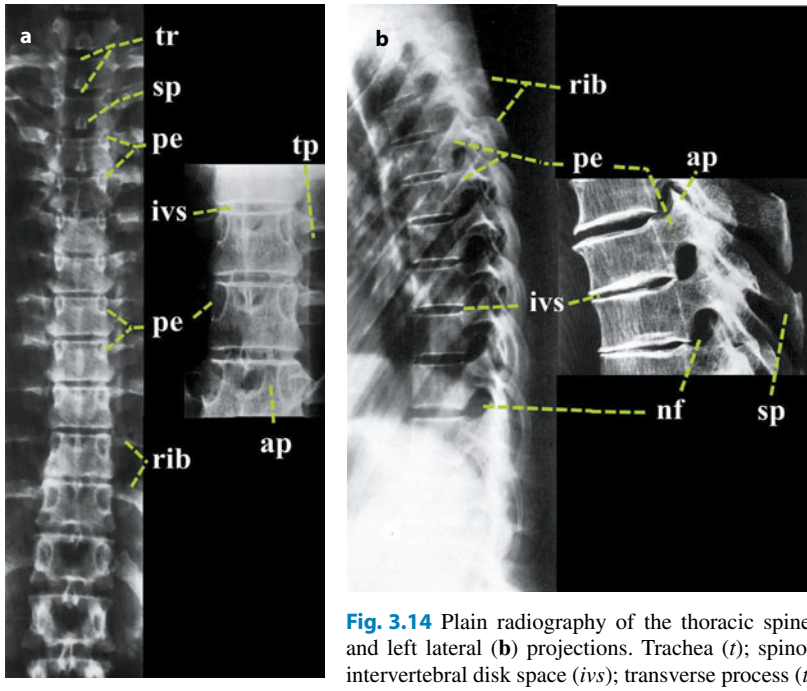

Fig. 3.14 Plain radiography of the thoracic spine showing anteroposterior (**a**) and left lateral (**b**) projections. Trachea (*t*); spinous process (*sp*); pedicle (*pe*); intervertebral disk space (*ivs*); transverse process (*tp*); articular process (*ap*); vertebral body (*vb*); neural foramen (*nf*)

are often concave. The image of the VB can be deformed depending on the angle of incidence of the radiation beam. The peduncles are projected on the supero-external angles of the soma and aligned symmetrically in the AP direction, thereby defining the outer boundaries of the spinal canal. The inter-pedicular distance increases gradually from L1 to L5.

Recognizing the inter-apofiso–laminar space (a diamond shape flanked by two adjacent vertebrae) is important. Its boundaries are arranged from the bottom edge of the laminae and the spinous process of the vertebra above, laterally from the inner surface of the articular apophyses, and downwards from the upper edge of the laminae of the underlying vertebra. This airspace increases progressively in amplitude caudally and is important for evaluation of stenosis of the spinal canal (Fig. 3.15a). The interbody space is occupied by the intervertebral disk and looks like a transparent band when assessing the height. Sometimes, this transparency is reduced by disk calcification or increased in the presence of vacuolar degeneration by accumulation of gas in the disk.

LL projection (Fig. 3.15b): VBs have a quadrangular shape with a central portion of cancellous bone bounded by cortical bone. The front profile of the VB is, in general, straight or slightly concave forward; the posterior profile is concave (sometimes quite pronounced). The soma of L5 shows slight deformation of the posterior wedge. The pedicles overlap perfectly with the upper and lower edge, and are slightly concave. The posterior articular apophyses overlap with each other to form a column of relative opacity in which the superior and inferior processes can be recognized. The foramina are bordered on the posterior margin of the intervertebral disk and corresponding vertebral soma, posteriorly by the surface of the articular processes, up from the bottom edge of the vertebra above and below the upper edge of the one below.

LL projection: The neural foramina between L1 and L4 are displayed without deformation as a large oval shape that decrease progressively in size proceeding downwards and which have a small indentation caused by the posterior superior articular process of the underlying vertebra.

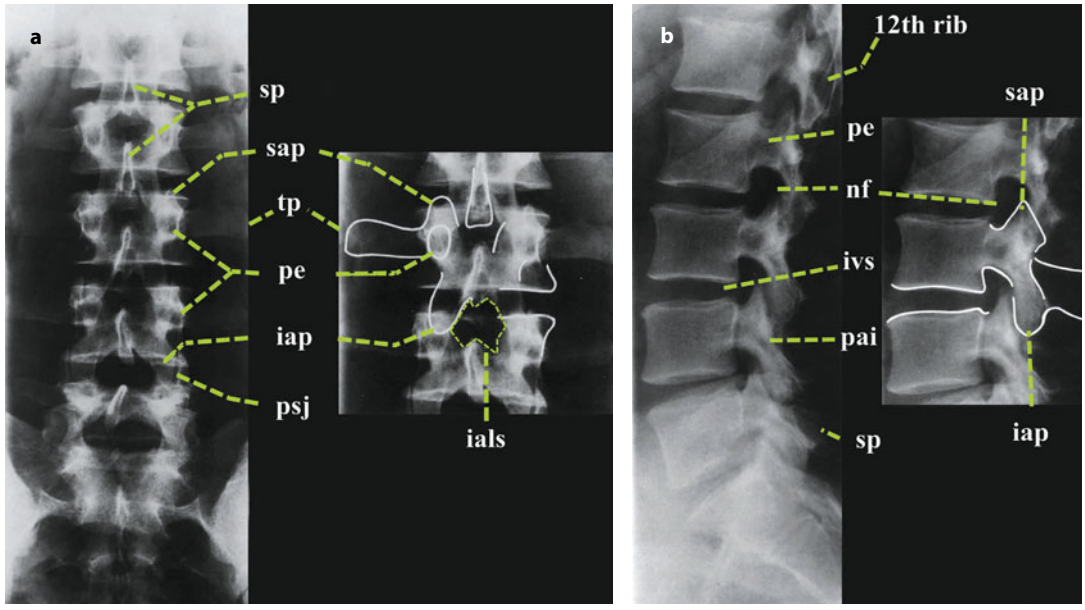

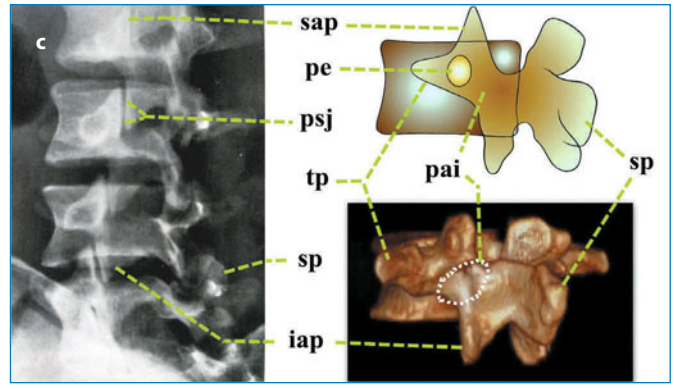

Fig. 3.15 Plain radiography of lumbosacral segments in anteroposterior (**a**), left lateral (**b**) and oblique projections with three-dimensional volume-rendered multidetector row CT reconstruction of the lumbar vertebra (**c**). Inter-apophyseal laminar space (*ials*); transverse process (*tp*); twelfth rib (12th rib); pedicle (*pe*); intervertebral disk space (*ivs*); spinous process (*sp*); inferior articular process (*iap*); superior articular process (*sap*); pars interarticularis (*pai*); vertebral body (*vb*); neural foramen (*nf*); posterior spinal facet joint (zygapophyseal) (*psj*)

At L5–S1 the foramen appears to be smaller and flattened because it has a different orientation than those situated above. Narrowing in the AP position of the foramina can result from congenital shortness of the pedicles, hypertrophy of the posterior facet joint, arthrosis, or degenerative spondylolisthesis. A reduction in height can be an indicator of disk degeneration (which undergoes thinning) or by an increase of the thickness of the pedicle.

The oblique view (Fig. 3.15c) is still used frequently in the lumbar spine for exploration of the posterior arch. It has the classic appearance of the "Scottie dog" in which the: face corresponds to the transverse apophysis; ear to the superior articular apophysis; eye to the pedicle; neck to the inter-joint isthmus; front leg to the inferior articular apophysis; body to the lamina. The main interest of this projection lies in the study of the isthmus inter-articular and posterior joints because the spacing and articular surface can be seen.

3.4.3.1 Anatomical Variations in the Lumbar Spine

During percutaneous treatment, to avoid complications or mistakes, knowing the anatomical variations in the lumbar spine is extremely important [12]. These variations are detailed in Table 3.1.

Table 3.1 Anatomical variations in the lumbar spine

- Costiform process at L1. The transverse apophysis of L1 can assume a morphology similar to that of a rib and be unilateral or bilateral.
- Persistence of accessory ossification nucleus. This is sometimes present in correspondence with the transverse processes or joints, which are situated distally.
- Persistence of the epiphyseal center of ossification. This is most often observed on the anterior superior margin of L1 or, more rarely, L2 and L3. It should not be confused with marginal bone trauma.
- Persistence of a "vascular window" of the vertebral body that is manifested as an area of segmental radio-transparency (front or back).
- Net linear opacities and somatic courses parallel to the plates with the same meaning as metaphyses of long bones, and which correspond to growth striae;
- Lumbar styloid apophysis. Corresponds to hypertrophy of the tubercle accessory located below the mammillary tubercle and behind the superior articular apophysis. On AP projection it appears as a bone of varying length originating (apparently) from the superior articular apophysis heading down and out (where it crosses the transverse process).
- Constitutional hypertrophy of the pedicles or vertebral joints that can cause narrowing of the conjugation foramen.
- Presence of "eyes" in the classic image of a Scottie dog caused by hypertrophy of the mammillary process.
- Partial or complete sacralization of L5. This is very common and characterized by a transverse mega-apophysis (unilateral or bilateral L5) associated with neo-articulation with the sacral bone. The distinction between a sacralization of L5 or S1 lumbarization is not straightforward and may require an exact definition for the full count of the individual vertebrae of the entire vertebral spine.

3.5 Access Routes and Patient Positioning for Percutaneous Treatments

The percutaneous route is chosen based on the location and depth of the target so as to reach it with a route as short as possible while respecting sensitive anatomical structures. Recognition of the main landmarks in the skin (normally used for the execution of conventional radiography) which correspond in depth to a given vertebral spine are useful for the choice of the decubitus position (Fig. 3.16). The prone position is the most commonly used and allows access to almost any target in the dorsal and lumbosacral segments. Placement of a pillow under the abdomen reduces lumbar lordosis, and facilitates access to the most caudal intervertebral disks and the lower termination of the vertebral posterior articular synovium. The entry point of the skin for the decubitus position is, in general, posterolateral and at a variable distance from the interspinous line (or may coincide with this line in specific cases) (Fig. 3.17a). The lateral decubitus position is sometimes employed, especially in the lumbosacral segments, to reach the intervertebral disk [13–15]. Also, in this case, placement of a pillow under the side support can align the vertebrae in the median plane (Fig. 3.17b). For percutaneous treatment at the cervical spine, a supine decubitus position with slight hyperextension of the head is the most commonly used. The salience of the muscle bundle of the sternomastoid is the reference for access to lower-middle cervical vertebrae (Fig. 3.18).

The mouth as the "gateway" to the second cervical vertebra was employed by surgeons of various disciplines for many years [16–19]. More recently it has been used to undertake percutaneous vertebroplasty due to vertebral collapse caused by osteoporosis or cancer. Vertebroplasty of C2 can be achieved with an equal probability of success under radiographic or CT guidance [20–24].

Accesses route for percutaneous procedures that can create particular difficulties are the high thoracic region and cervical–thoracic transition. This is due to the overlap of the scapulohumeral crack and small size of the pedicles of the upper thoracic vertebrae. Good visualization of the vertebrae and the paraspinal soft tissue is of fundamental importance because of the close relationship with the spinal canal, pleural cavity

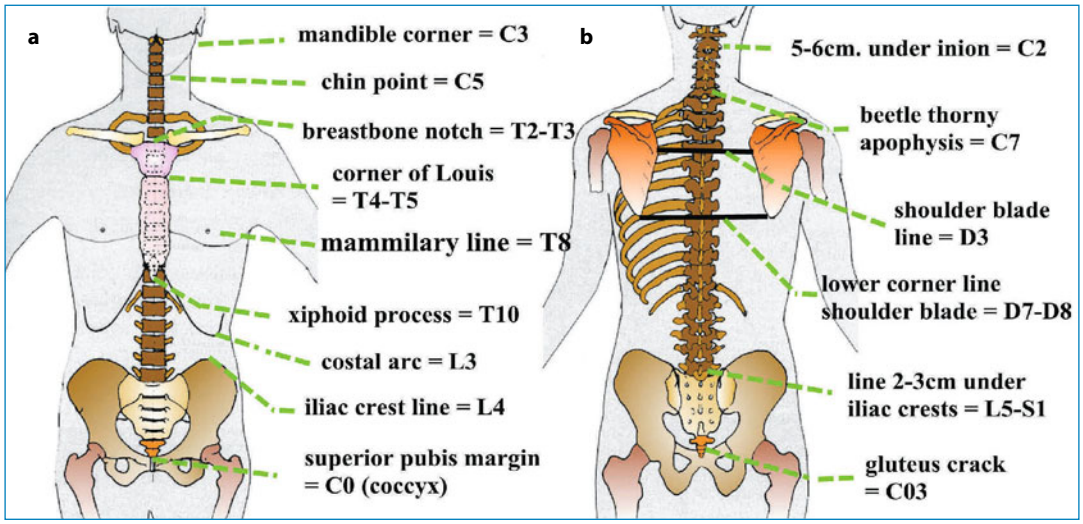

Fig. 3.16 Points of reference to locate the vertebral level in skin according to anterior (**a**) and posterior (**b**) projections

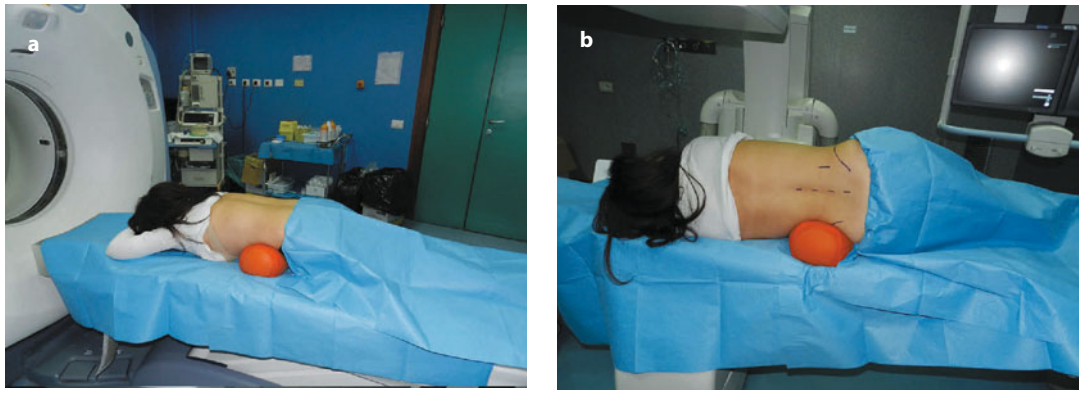

Fig. 3.17 Patient positioning for access to the thoracic–lumbar–sacral region. Supine (**a**) and lateral decubitus (**b**) positions are shown

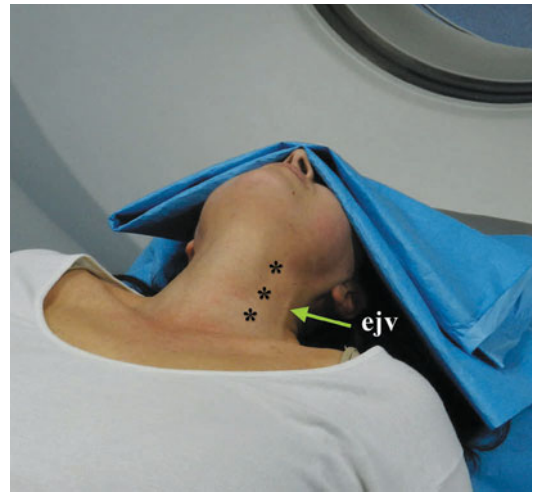

Fig. 3.18 Patient positioning for percutaneous access to the cervical spine (C3–C7). External jugular vein (*ejv*)

and major vascular structures. To improve the accuracy of radiological visualization, various measures should be adopted, including ensuring that the arms are abducted and elbows flexed forward if the procedure is carried out under sedation. This results in lowering of the shoulder blades, which greatly reduces the image overlay in the LL projection and good visualization of T2, resulting in easier undertaking of percutaneous treatments [25].

When using CT guidance for percutaneous treatments, the "swimmer's position" can be adopted to reduce artifacts from "hardening" of the radiation beam present at cervicothoracic junction (especially in subjects with short or thick necks). The patient is placed supine on the CT table and one of his/her arms placed behind the head. This position has been shown to elicit a net reduction of artifacts with clearer evidence of pathological processes at the base of the neck and cervicothoracic junction [26–27].

References

1. Rabischong R, Salvolini U (1987) La "logica" anatomica dell'imaging vertebro-nevrassiale. In: Pistolesi GF, Bergamo Andreis IA (eds) L'imaging diagnostico del rachide. Cortina, Verona 110–120
2. Rabischong P (1989) Anatomie functionnelle du rachis et de la moelle. In: Manelfe C (ed) Imagerie du rachis et de la moelle. Vigot, Paris, 109–134
3. Koritke JG, Sick H (1983) Atlas of sectional human anatomy. Urban & Schwarzenberger, Baltimore-Munich, pp 65–95
4. Zaccaria F, Marinozzi G, Nesci E, Santoro A (1973) Atlante fotografico a colori di Anatomia macroscopica dell'uomo. Dr. F. Vallardi Società Editrice Libraria, Roma, pp 75–90
5. Lambertini G (1968) Manuale di Anatomia dell'uomo. Piccin Editore, Padova pp 115–135
6. Newton TH, Potts DG (eds) (1983) Modern neuroradiology volume 1: computed tomography of the spine and spinal cord. Clavadel Press, San Anselmo
7. Jinkins JR (2000) Atlas of neuroradiologic embryologic anatomy and variants. Lippincott Williams & Wilkins, Edinburgh, pp 15–25
8. Harnsberger HR, Salzman KL, Osborn AG, Ross JS, Macdonald AJ (2006) Diagnostic and surgical imaging anatomy: brain, head and neck, spine. Amirsys, Salt Lake City, pp 2–4
9. Ebraheim NA, Haman ST, Xu R, Yeasting R (1998) The anatomic location of the dorsal ramus of the cervical nerve and its relation to the superior articular process of the lateral mass. Spine 23:1968–1971
10. Runge M (1988) Rachis dorsal. Encycl Med Chir (Paris, France), Radiodiagnostic 1, 30650 B10.12-1988
11. Runge M (1988) Rachis lombar. Examen radiographique standard. Encycl Med Chir (Paris, France), Radiodiagnostic 1, 30600 A10.12-1988
12. Runge M (1988) Rachis lombar. Données anatomique. Encycl Med Chir (Paris, France), Radiodiagnostic 1, 30650 A10.12-1988
13. Fabris G, Lavaroni A, Leonardi M (1991) Discography. Del Centauro, Udine
14. Benoist M, Deburge A, Busson J. (1984) La chimonucleolyse dans le traitment des sciatique par hernie discale. La Press Medicale 13:733–736
15. Boneville J-F, Clarisse J (1984) Radiologie interventionelle. In: Manelfe C (ed) Imagerie du rachis et de la moelle. Vigot, Paris, 761–784
16. Bonney G, Williams JP (1985) Trans-oral approach to the upper cervical spine. A report of 16 cases. J Bone Joint Surg Br 67:691–698
17. Merwin GE, Post JC, Sypert GW (1991) Transoral approach to the upper cervical spine. Laryngoscope 101:780–784
18. Menezes AH, VanGilder JC (1988) Transoral–transpharyngeal approach to the anterior craniocervical junction: ten-year experience with 72 patients. J Neurosurg 69:895–903
19. Fang HS, Ong GB, Hodgson AR (1964) Anterior spinal fusion: the operative approaches. Clin Orthop 35:16–33
20. Jensen ME, Evans AJ, Mathis JM, Kallmes DF, Cloft HJ, Dion JE (1997) Percutaneous polymethylmethacrylate vertebroplasty in the treatment of osteoporotic vertebral body compression fractures: technical aspects. Am J Neuroradiol 18:1897–1904
21. Martin JB, Gailloud P, Dietrich PY et al (2002) Direct transoral approach to C2 for percutaneous vertebroplasty. Cardiovasc Intervent Radiol 25:517–519
22. Gailloud P, Martin JB, Olivi A, Gailloud P, Martin JB (2002) Transoral vertebroplasty for a fractured C2 aneurysmal bone cyst. J Vasc Interv Radiol 13:340–341
23. Tong FC, Cloft HJ, Joseph GJ Rodts GR, Dion JE (2000) Transoral approach to cervical vertebroplasty for multiple myeloma. Am J Roentgenol 175:1322–1324
24. Arra S. Reddy, Mary Hochman, Shaun Loh et al (2005) CT guided direct transoral approach to C2 for percutaneous vertebroplasty. Pain Physician 8:235–238
25. Bayley E, Clamp J, Bronek MB (2009) Percutaneous approach to the upper thoracic spine: optimal patient positioning. Eur Spine J 18:1986–1988
26. Kane AG, Reilly KC, Murphy TF (2004) Swimmer's CT: improved imaging of the lower neck and thoracic inlet. Am J Neuroradiol 25:859–862
27. Bartynski WS Whitt DS, Sheetz MA, Jennings RB, Rothfus WE (2007) Lower cervical nerve root block using CT fluoroscopy in patients with large body habitus: another benefit of the swimmer's position. Am J Neuroradiol 28:706–708